Lysophosphatidic Acid Induces ECM Production via Activation of the Mechanosensitive YAP/TAZ Transcriptional Pathway in Trabecular Meshwork Cells

Leona T. Y. Ho,[1] Nikolai Skiba,[1] Christoph Ullmer,[2] and Ponugoti Vasantha Rao[1,3]

[1]Department of Ophthalmology, Duke University School of Medicine, Durham, North Carolina, United States
[2]Roche Pharma Research and Early Development, Roche Innovation Center Basel, F. Hoffmann-La Roche Ltd., Basel, Switzerland
[3]Department of Pharmacology and Cancer Biology, Duke University School of Medicine, Durham, North Carolina, United States

Correspondence: Ponugoti Vasantha Rao, Department of Ophthalmology, Duke University School of Medicine, Durham, NC 27710, USA; p.rao@duke.edu.
Christoph Ullmer, Roche Pharma Research and Early Development, Roche Innovation Center Basel, F. Hoffmann-La Roche Ltd., Basel, Switzerland; Christoph.ullmer@roche.com.

Submitted: December 21, 2017
Accepted: March 10, 2018

Citation: Ho LTY, Skiba N, Ullmer C, Rao PV. Lysophosphatidic acid induces ECM production via activation of the mechanosensitive YAP/TAZ transcriptional pathway in trabecular meshwork cells. *Invest Ophthalmol Vis Sci*. 2018;59:1969–1984. https://doi.org/10.1167/iovs.17-23702

Purpose. Lysophosphatidic acid (LPA), a bioactive lipid, has been shown to increase resistance to aqueous humor outflow (AH) through the trabecular meshwork (TM). The molecular basis for this response of the TM to LPA, however, is not completely understood. In this study, we explored the possible involvement of mechanosensitive Yes-associated protein (YAP) and its paralog, transcriptional coactivator with PDZ-binding domain (TAZ), transcriptional activation in extracellular matrix (ECM) production by LPA-induced contractile activity in human TM cells (HTM).

Methods. The responsiveness of genes encoding LPA receptors (*LPARs*), LPA hydrolyzing lipid phosphate phosphatases (*LPPs*), and the LPA-generating autotaxin (*ATX*) to cyclic mechanical stretch in HTM cells, was evaluated by RT-quantitative (q)PCR. The effects of LPA and LPA receptor antagonists on actomyosin contractile activity, activation of YAP/TAZ, and levels of connective tissue growth factor (CTGF), and Cyr61 and ECM proteins in HTM cells were determined by immunoblotting, mass spectrometry, and immunofluorescence analyses.

Results. Cyclic mechanical stretch significantly increased the expression of several types of LPARs, LPP1, and ATX in HTM cells. LPA and LPA receptor–dependent contractile activity led to increases in both, the protein levels and activation of YAP/TAZ, and increased the levels of CTGF, Cyr61, α-smooth muscle actin (α–SMA), and ECM proteins in HTM cells.

Conclusions. The results of this study reveal that LPA and its receptors stimulate YAP/TAZ transcriptional activity in HTM cells by modulating cellular contractile tension, and augment expression of CTGF that in turn leads to increased production of ECM. Therefore, YAP/TAZ-induced increases in CTGF and ECM production could be an important molecular mechanism underlying LPA-induced resistance to AH outflow and ocular hypertension.

Keywords: trabecular meshwork, lysophosphatidic acid, cell adhesion, contraction, mechanotransduction

Homeostasis of aqueous humor (AH) drainage through the conventional and nonconventional outflow pathways is crucial for maintenance of IOP. Blockage of AH drainage can lead to increased IOP or ocular hypertension, which is a dominant risk factor for glaucoma, a leading cause of irreversible blindness.[1] It is now well understood that various external factors present in the AH act through cell surface receptors to modulate AH outflow via the trabecular or conventional pathway, which accounts for the majority of AH drainage in humans.[2,3] Importantly, the levels of certain external factors including TGF-β, endothelin-1, and connective tissue growth factor (CTGF) have been reported to be elevated in the AH of glaucoma patients, while in vitro studies demonstrate that perfusion with and overexpression of these factors increased resistance to AH outflow and elevated IOP through different cellular and molecular mechanisms.[3–8] Prior studies from our laboratory have also reported that lysophosphatidic acid (LPA), which is produced extracellularly by autotaxin/lysophospholipase-D, regulates AH outflow through the trabecular pathway.[9,10] Moreover, the levels of LPA and autotaxin (ATX), and activity of ATX in the AH of glaucoma patients and ocular hypertensive mice have been reported to be elevated suggesting that dysregulated LPA-mediated physiology is very likely involved in ocular hypertension.[10–12] However, the molecular basis for LPA-induced resistance to AH outflow is not thoroughly understood.

LPA is predominantly produced by ATX from its substrate lysophosphatidylcholine (LPC), and is involved in regulation of various cellular activities, including cell proliferation, differentiation, survival, migration, and contraction, and in the pathobiology of cancer, fibrosis, and several other diseases dealing with chronic inflammation.[13–15] LPA is degraded by lipid phosphate phosphatases (LPPs) and other enzymes,[16] and evokes biological effects through multiple G-protein coupled receptors (LPARs). There are six well characterized LPAR genes encoding proteins LPAR1-6, respectively,[13] that couple to various G-proteins (e.g., Gα12/13, Gαq/11, and Gαi and Gαs) in order to regulate intracellular signaling pathways, including Rho GTPase, phospholipase C, protein kinase C, adenylate cyclase, and calcium release.[13,17,18] In human trabecular

meshwork (HTM) cells, LPA has been shown to regulate actin cytoskeletal organization, cell contraction, and adhesion by activating both Rho GTPase and calcium signaling.[9,19,20] Moreover, LPA has also been shown to regulate production of certain extracellular matrix (ECM) proteins, expression of α-smooth muscle actin (α-SMA) and CTGF in TM cells, and cell plasticity by stimulating activation of the serum response factor (SRF) and myocardin-related transcription factor (MRTF), and through other mechanisms as well.[2,21,22] Although CTGF, a well-recognized fibrogenic factor that acts in concert with TGF-β or independently, is known to regulate ECM production, actomyosin organization, and fibrogenic activity,[23–26] the question of whether CTGF expression is regulated by LPA-dependent mechanosensitive transcriptional mechanism(s) in HTM cells, has not been explored.[27] Mechanical stretch, ECM stiffness, and elevated IOP have been shown to upregulate CTGF expression in HTM cells and tissue, respectively, indicating existence of a plausible link between the mechanotransducing transcriptional pathways and CTGF expression.[28–30]

Gene expression regulated by Yes-associated protein (YAP) and its paralog, transcriptional coactivator with PDZ-binding domain (TAZ) is considered to play a vital role in organ growth, size, cell proliferation, and survival, and is involved in the pathobiology of various diseases including cancer and fibrosis.[31–34] Importantly, the activity of YAP/TAZ transcription factors has been demonstrated to be regulated by cell morphology, cell-cell contact, actin cytoskeletal polymerization, ECM stiffness, contractile activity and focal adhesion-driven force, cell-matrix interaction, metabolic activity, and by Rho GTPase.[34–38] YAP and TAZ are known to regulate expression of the CNN family of genes including CTGF and Cyr61, which are matricellular proteins participating in fibrotic activity.[29,39,40] Along with the Hippo pathway, several different upstream cellular mechanisms also regulate activation of YAP/TAZ through protein phosphorylation-dephosphorylation–mediated differential distribution of YAP/TAZ between the cell cytosol and nuclear fractions.[31,34] Unphosphorylated YAP and TAZ translocate to the nucleus and activate transcription by binding to different transcriptional regulators including TEAD, RUNX, and SMADS.[31,32] LPA has been demonstrated to be capable of regulating YAP/TAZ activity via its cognate receptors and their effects on actin cytoskeletal polymerization, actomyosin driven cellular contraction, and Rho GTPase activity.[27,34,41–43] MRTF-A, which is activated by LPA and Rho GTPase, was also very recently shown to interact with YAP and regulate the YAP-dependent transcriptional response independent of large tumor suppressor (LATS) kinases.[44] Additionally, dysregulated levels of LPA, LPARs, and ATX have also been reported to impact fibrosis in different tissues and cell types.[45–49] The role of LPA in regulation of YAP/TAZ activity in HTM cells however, has not been investigated. Therefore, in this study, we examined the interrelationship between LPA- and LPAR-induced contractile activity, YAP/TAZ activation, CTGF expression, and ECM production in HTM cells, in the context of AH outflow and ocular hypertension.

Materials and Methods

Chemicals

LPA (Cat. no. 10010093; Cayman Chemical, Ann Arbor, MI, USA), Y27632 (Cat. no. 1254; Tocris Bioscience, Bristol, UK), GF109203X and ML-7 (Cat. no. G2911 and Cat. no. I2764, respectively; Sigma-Aldrich Corp., St. Louis, MO, USA) were purchased from the respective commercial sources. LPA receptor antagonists, AM095, Cpd 35, and Ki16425 were obtained from F. Hoffmann-La Roche Ltd. (Basel, Switzerland).

HTM Cell Culture

Human primary TM cells were derived from TM tissue isolated from donor corneal rings (donors aged between 19 and 67 years) used for corneal transplantation at the Duke Ophthalmology Clinical Service, as previously described.[22] Cells were cultured at 37°C under 5% CO_2, in Dulbecco's modified Eagle's medium (DMEM; Invitrogen, Carlsbad, CA, USA) containing 10% fetal bovine serum (FBS), glutamine (4 mM), and antibiotics (penicillin, 100 U/mL; streptomycin 100 μg/mL). All experiments were conducted using confluent HTM cell cultures between 3 and 6 passages, and cells were serum-starved for 24 hours prior to treatment with various agents.

Cyclic Mechanical Stretch

Primary cultures of HTM cells were plated onto BioFlex six-well plates precoated with collagen type I (Flexcell International Corp., Burlington, NC, USA). As the cells reached confluence, cultured medium was switched to serum-free, phenol-free DMEM, and cells were subjected to cyclic mechanical stretch (15% stretching, 1 cycle/sec) for 24 hours, using the computer-controlled vacuum-operated FX-3000 Flexcell Strain Unit (Flexcell, Hillsborough, NC, USA), as we previously described.[10] Control cells were cultured under similar conditions with no mechanical force applied. RNA was extracted from the cells and analyzed by RT-quantitative (q)PCR to monitor changes in level of expression of LPARs, LPPs, and ATX.

RT-PCR and RT-qPCR

Total RNA was extracted from confluent cultures of HTM cells using an RNeasy Micro kit (Qiagen, Valencia, CA, USA), according to the manufacturer's instructions. One microgram of total RNA was used to prepare complementary (c)DNA by reverse transcription. Expression of *LPARs*, *LPPs*, and *ATX* was determined by RT-PCR (C1000 Touch Thermocycler; Bio-Rad Laboratories, Hercules, CA, USA). The reaction conditions included denaturation at 95°C for 30 seconds, annealing at 60°C for 30 seconds, and extension at 72°C for 60 seconds. The cycle was repeated 30 times with a final step at 72°C for 5 minutes. The primer sequences used in this study and the expected size of amplified DNA fragments are listed in Table 1. The resulting DNA products were separated on 1.5% agarose gels and visualized with GelRed Nucleic Acid Stain (Biotium, Hayward, CA, USA) using a Fotodyne Transilluminator (Fotodyne, Inc., Hartland, WI, USA). Control reactions containing no reverse transcriptase were run simultaneously.

Real-time qPCR was performed using a CFX 96-RealTime System (Bio-Rad Laboratories), and the cDNA content of control and stretched samples for RT-qPCR reactions was normalized to Glyceraldehyde 3-phosphate dehydrogenase (GAPDH) expression. The PCR master mix consisted of 1-μL template cDNA in 20 μL reaction, 10 μL 2 × iQ SYBR Green supermix (Bio-Rad Laboratories), and 500 nM each of a gene-specific oligonucleotide pair. RT-qPCR reactions were performed in triplicate using the following protocol: 95°C for 3 minutes followed by 39 cycles of the following sequence: 95°C for 10 seconds (denaturation), 58°C for 30 seconds (annealing), and 72°C for 15 seconds (extension). An extension step was used to measure the increase in fluorescence and melting curves were obtained immediately after amplification. The fold difference in expression of *LPARs*, *LPPs*, and *ATX* gene

Investigative Ophthalmology & Visual Science

Table 1. Oligonucleotide Primers Used in RT-PCR and RT-qPCR Analyses

Gene Name	Forward Primer	Reverse Primer	Product Size, bp
LPAR1	GGTGGTCATTGTGGTCATCT	CATAGTCCTCTGGCGAACATAG	217
LPAR2	TTCCACCAGCCCATCTA	CACCATGAGGAAGACAA	429
LPAR3	GAGGGTGACACTGCTCATTT	CCTCGTCCTTGTAGGAGTAGAT	467
LPAR4	GGTGCTGTCTACAGTGTTGTAT	GCTCCCATAGATGTTGGTAAGG	249
LPAR5	GTGCTTCGTGCCCTACAA	GTGTGAAGGAAGACAGAGAGTG	359
LPAR6	CTACCCACTCTCAGGGTAACA	GCTGCCACTACTGAGCAATTA	337
LPP1	ACGTCTGAGGCCCAACTTC	GAAGTGAGGCCGCAGTCTGCCTATTG	365
LPP2	GCGTCTGAGGCCCAACTTC	CGTTCCAGATCCTCCTCCT	426
LPP3	CGCGGTCGATTCAGAAC	GCGAGACAGTCCCGTGTAGA	395
ATX	CGGATTCCTCTTTCCTCCTTATC	GCTGGTGATGATGCTGTAGT	289
GAPDH	TGCACCACCAACTGCTTAGC	GGCATGGACTGTGGTCATGAG	452

between control and cyclic stretch–treated (stretched) samples were calculated by the comparative threshold (Ct) method, as described by the manufacturer (CFX Manager; Bio-Rad Laboratories).

Myosin Light-Chain Phosphorylation

Myosin light-chain (MLC) phosphorylation status in HTM cells was determined as we described previously.[22] Briefly, serum-starved cultures of HTM cells were treated with LPA or other agents and were extracted with 10% ice-cold trichloracetic acid and 0.5M dithiothreitol (DTT). Precipitates obtained after centrifugation at 16,000*g* were dissolved in 8 M urea buffer (20 mM Tris, 23 mM glycine, 10 mM DTT saturated in sucrose) and containing protease and phosphatase inhibitor cocktails, and briefly sonicated. Protein concentration was determined using a BCA protein assay kit (Pierce Chemical Co., Rockford, IL, USA), according to manufacturer's protocol. Lysates (10 μg per sample) were subjected to urea/glycerol-polyacrylamide gel electrophoresis and Western blot analysis with rabbit polyclonal antibody directed against di-phospho-MLC (Thr18/Ser19, 1:1000 dilution, Cat. no. 3674; Cell Signaling Technology, Danvers, MA, USA), as described previously.[21] Data were normalized to total MLC. MLC antibody (1:1000 dilution) was purchased from Cell Signaling (Cat. no. 3672).

Immunoblotting Analysis

Following completion of various study treatments, HTM cells were lysed with hypotonic buffer (10 mM Tris buffer, pH 7.4, containing 0.2 mM $MgCl_2$, 5 mM N-ethylmaleimide, 2.0 mM Na_3VO_4, 10 mM NaF, 60 μM PMSF, 0.4 mM iodoacetamide and supplemented with protease and phosphatase inhibitor cocktail). The cell lysates were then gently sonicated, followed by low-speed centrifugation (800*g*) for 15 minutes at 4°C, and the resulting supernatant samples (10 μg lysate protein) were resolved on 8% to 12% SDS-PAGE and transferred to nitrocellulose membranes, as previously described.[21] Membranes were probed with one of the following antibodies for 18 hours at 4°C: phospho-FAK (Tyr 397) (p-FAK) (rabbit polyclonal; 1:2000 dilution; Cat. no. 700255; Thermo Fisher Scientific): phospho-YAP (Ser 127) (D9W2I) (p-YAP) (rabbit polyclonal; 1:1000 dilution; Cat. no. 13008; Cell Signaling Technology, Danvers, MA, USA): YAP (rabbit polyclonal; 1:1000 dilution; Cat. no. 4912; Cell Signaling Technology): YAP/TAZ (D24E4) (rabbit polyclonal; 1:1000 dilution; Cat. no. 8418; Cell Signaling Technology); phospho-TAZ (Ser 89) (p-TAZ) (rabbit polyclonal; 1:500 dilution; Cat. no. sc-17610-R; Santa Cruz Biotechnology, Santa Cruz, CA, USA): CTGF (rabbit polyclonal; 1:1000 dilution; Cat. no. ab6992; Abcam, Cambridge, MA, USA); Cyr61 (A-10) (rabbit polyclonal; 1:500 dilution; Cat. no. sc-374129; Santa Cruz Biotechnology): α-SMA (mouse monoclonal; 1:1000 dilution; Cat. no. A2547; Sigma-Aldrich Corp.): fibronectin (rabbit polyclonal; 1:15,000 dilution; Cat. no. ab23750; Abcam): laminin-α (rabbit polyclonal; 1:1000 dilution; a gift from Harold P. Erickson (Department of Cell Biology, Duke University, Durham, NC, USA): collagen type I (rabbit polyclonal; 1:1000 dilution; Cat. no. 600-401-103-0-1; Rockland Immunochemicals, Inc., Limerick, PA, USA): MLC (rabbit polyclonal; 1:1000 dilution; Cell Signaling Technology): and GAPDH (mouse monoclonal antibody; 1:10,000 dilution; Cat. no. 60004-1-g; Proteintech Group, Inc., Rosemont, IL, USA). After washing away primary antibodies, nitrocellulose membranes were incubated with appropriate horseradish peroxidase–conjugated secondary antibodies (1:5000 dilution; Jackson Immuno Research, West Grove, PA, USA) for 2 hours at room temperature, and immunopositive protein bands were detected with an enhanced chemiluminescent substrate, as we described earlier.[22] Quantification was performed with ImageJ software (http://imagej.nih.gov/ij/; provided in the public domain by the National Institutes of Health, Bethesda, MD, USA), and results were normalized to the indicated loading controls.

Immunofluorescence Analysis

HTM cells were grown on 2% gelatin coated glass coverslips (12-well plates) until attainment of 70% top 80% confluency. Following treatments with the agent of interest in serum-free media, cells were washed twice with PBS and then fixed in 4% paraformaldehyde for 15 minutes. After fixing, washing, permeablization, and blocking were completed as we described earlier,[22] cells were incubated with Tetramethylrhodamine-phalloidin (1:500 dilution; Cat. no. P1951; Sigma-Aldrich Corp.) for 30 minutes to detect F-actin organization, or for 2 hours at room temperature with antibodies directed against YAP (1:200 dilution), YAP/TAZ (1:200 dilution), α-SMA (mouse monoclonal antibody conjugated with Cy3, at a 1:500 dilution; Cat. no. C6198; Sigma-Aldrich Corp.), fibronectin (1:200 dilution), laminin (1:200 dilution), or collagen type I (1:200 dilution). After thoroughly washing away the primary antibodies, specimens were incubated with the appropriate Alexa fluor-conjugated secondary antibody for 2 hours at room temperature as described previously.[22] Coverslips were mounted onto glass slides using Shandon Immu-Mount (Thermo Fisher Scientific), then viewed and imaged using a Nikon Eclipse 90i confocal laser-scanning microscope (Melville, NY, USA). Controls for

Investigative Ophthalmology & Visual Science

background nonspecific fluorescence consisted of HTM cells carried simultaneously through the same treatment protocol, using only the appropriate fluoroprobe conjugated secondary antibodies.

Extraction of ECM-Enriched Fraction

HTM cells were cultured in 100 × 20-mm plastic cell culture dishes in DMEM containing 10% FBS and antibiotics. After reaching confluence, cells were serum starved for 24 hours and treated with LPA (5 μM added twice a day) for 48 hours. Cell monolayers were decellularized from culture plates and the ECM-enriched fraction was extracted, as we described previously.[50] The ECM extract was solubilized with 200 μL of SDS buffer (5% SDS, 10% glycerol, 60 mM Tris-HCl, pH 6.8, supplemented with protease and phosphatase inhibitor cocktail), followed by a 5-minute incubation with gentle mixing at 95°C, then centrifuged at 16,000*g* for 10 minutes. The supernatant containing SDS soluble ECM proteins was collected and placed on ice. The pellet (SDS-insoluble fraction) was further resuspended in 200 μL urea buffer (8 M urea, 4% SDS, 60 mM Tris-HCl, 12.5 mM EDTA, supplemented with protease and phosphatase inhibitor cocktail), incubated at room temperature for 30 minutes, and centrifuged at 16,000*g* for 5 minutes at 4°C. The supernatant from this step was combined with the SDS soluble fraction to generate a 'SDS/urea soluble fraction', which was stored at –80°C until further analysis. The remaining pellet (SDS/urea insoluble fraction) was resuspended in urea buffer and gently sonicated. The protein concentration of both SDS/urea soluble and SDS/urea insoluble ECM samples was determined using BCA protein assay kit (Pierce Biotechnology, Rockford, IL, USA).

In-Gel Protein Digestion

SDS/urea soluble-ECM–enriched samples were separated on gradient (4%–20%) Tris-Glycine gels (Bio-Rad Laboratories) using MOPS-SDS running buffer (Invitrogen). The gels were stained overnight with Gel Code blue stain reagent (Pierce Biotechnology) and destained with deionized water. Protein bands were then excised from the gel and subjected to in-gel tryptic digestion using Trypsin/Lys-C mix (Promega, Madison, WI, USA) and the In-Gel Tryptic digestion kit (Pierce Biotechnology), per manufacturer's protocol. This digestion process included reduction and alkylation of protein samples. Trypsin digested ECM peptides were extracted from gel slices using 250 μL of 50% acetonitrile/1% formic acid at 37°C for 40 minutes. These peptide samples were transferred into a fresh 1.5-mL centrifuge tube, vacuum-dried, and resuspended in 10 μL of 0.1% formic acid.

Magnetic Bead Isolation

For in-solution trypsin digestion, we employed the magnetic bead method, as we described previously based on Maddala et al.,[50] and Hughes et al.[51] Briefly, the SDS/urea insoluble-ECM–enriched derived from both control and LPA-treated samples, were solubilized in 100 μL of 100 mM Tris–HCl (pH 8) buffer containing 2% SDS and 10 mM DTT, and alkylated with iodoacetamide (25 mM) by incubating in the dark at room temperature for 1 hour, after which the reaction was quenched with 50 mM DTT. Two microliters of premixed paramagnetic beads (10 μg Sera-Mag Speed Beads A and 10 μg Sera-Mag Speed Beads B; GE Pharmaceuticals) were added to the alkylated protein preparation, which was then acidified with 0.25% formic acid (pH <3), followed by an equal volume of 100% acetonitrile and incubation for 10 minutes at room temperature. A magnetic rack was used to capture the beads and discard supernatants. The beads were rinsed with 70% ethanol followed by acetonitrile. A Trypsin/Lys-C mix in 50 mM ammonium bicarbonate pH 8, was added to the beads and incubated overnight at 37°C. The following day, acetonitrile was added (>95%) to the samples and incubated for 10 minutes at room temperature. Samples were placed on the magnetic rack to capture the beads and supernatants were discarded. The beads were rinsed again with acetonitrile and 20 μL of 2% dimethyl sulfoxide and 0.2% formic acid were added to the beads and incubated for 5 minutes. The supernatants were collected, while the beads were incubated further with 20 μL of 0.2% formic acid for 5 minutes at room temperature. The supernatants from each sample were combined, vacuum-dried, and resuspended in 10 μL of 0.1% trifluoroacetic acid containing 3% acetonitrile.

Mass Spectrometry

The tryptic digest samples (3 μL) were analyzed by liquid chromatography–tandem mass spectrometry (LC-MS/MS) using a nano Acquity UPLC system coupled to a Synapt G2 HDMS mass spectrometer (Waters Corp., Milford, MA, USA) as we described earlier.[50] Briefly, peptides were initially trapped on a 180 μm × 20-mm Symmetry C18 column (at the 5 μL/min flow rate for 3 minutes in 99.9% water, 0.1% formic acid) and separated on a 75 μm × 150-mm column filled with the 1.7 μm C18 BEH resin (Waters Corp.), using a 6% to 30% acetonitrile gradient with 0.1% formic acid for 1.5 hour at a flow rate of 0.3 μL/min at 35°C. Eluted peptides were sprayed into the ion source of Synapt G2 using the 10-μm PicoTip emitter (Waters Corp.) at the voltage of 2.5 kV.

For each sample we conducted a data-dependent analysis (DDA) using a 0.8-second MS scan followed by MS/MS acquisition on the top four ions with charge greater than one. MS/MS scans for each ion used an isolation window of approximately 3 Da, a maximum of 2 sec/precursor, and dynamic exclusion for 90 seconds within 1.2 Da. DDA data were converted to searchable files using ProteinLynx Global Server 2.5.1 (Waters Corp.) and searched against the human UniProt database (September 2015 release; Cambridge, UK), using Mascot server 2.5 with the following parameters: maximum one missed cleavage site, carbamidomethylation at Cys residues as fixed modification, and Met oxidation, Asn, and Gln deamidation as variable modifications. Precursor ion mass tolerance was set to 20 ppm, while fragment mass tolerance to 0.2 Da. Mascot data were imported into Scaffold 4.4 (Proteome Software, Inc., Portland, OR, USA) to arrange all the data sets, identify a false discovery rate for protein identification, group proteins, and perform spectral counting–based protein quantification. Acceptance criteria for protein identification required identification at least two peptides for each protein with a confidence interval percentage over 99%, corresponding to a false discovery rate of 1%. Complete MS analysis was performed with two independently obtained SDS/urea soluble and SDS/urea insoluble ECM preparations.

Data Analysis

All data are expressed as means ± SEM for at least four independent experiments unless otherwise mentioned. Statistical analysis was performed using one-way ANOVA with Bonferroni's multiple comparison test for comparing within groups, and Student's *t*-test for statistical comparisons between two groups. A P value ≤ 0.05 was used to identify statistical significance.

Investigative Ophthalmology & Visual Science

Results

Mechanical Stretch-Mediated Upregulation of Expression of *LPARs*, *LPPs*, and *ATX* Expression in HTM Cells

LPA is involved in a wide range of biological events, acting through various G-protein coupled receptors to regulate several intracellular signaling pathways.[13,18,52] Because extracellular LPA has been shown to control cell contractile, adhesive, and mechanosensing activities,[18,19,52,53] we initially asked whether mechanical stretch of HTM cells influences the expression of LPA-sensing LPARs, LPA-degrading enzymes LPPs, and the LPA-generating enzyme ATX. For this, confluent HTM cells maintained at 37°C under serum-free conditions were subjected to cyclic mechanical stretch (15% stretch) for 24 hours. Control cells were cultured under identical conditions but were not subjected to cyclic mechanical stretch. Following completion of stretch, total RNA was extracted from cells and gene expression evaluated by RT-qPCR. The specificity of oligonucleotide primer sets used to amplify the expression of *LPAR1*, *2*, *3*, *4*, and *6*, *LPP1*, *2*, and *3*, and *ATX* was confirmed by running RT-PCR reactions using RNA derived from two independent HTM cell strains cultured from TM tissue obtained from 19- and 51-year-old human donor eyes. As shown in Figure 1A, HTM cells express all *LPARs* (*LPAR1*, *2*, *3*, *4*, and *6*) except *LPAR5*, *LPP1*, *2*, and *3*, and *ATX*. Expression of LPAR4 was noted to be weak in HTM cells, relative to the expression levels for *LPAR1*, *2*, *3*, and *6*. PCR products were sequenced to confirm specificity. Under cyclic mechanical stretch, expression of *LPAR1*, *3*, *4*, *LPP1*, and *ATX* was significantly increased in HTM cells compared with non-stretched controls (Fig. 1B). Data interpretation was based on the mean of six replicate analyses.

Involvement of Protein Kinase C, Rho Kinase, and Myosin Light Chain Kinase in LPA-Induced Contractile Activity in TM Cells

To explore the role of contractile and cell adhesive activity driven cellular tension in regulating mechanosensitive transcriptional activity in HTM cells, we initially examined LPA-mediated changes in actin stress fibers and MLC phosphorylation (a key determinant of myosin II–driven contractile force) in HTM cells, in the presence and absence of protein kinase C (PKC), Rho kinase, and MLC kinase (MLCK) inhibitors. Serum-starved HTM cells treated with LPA (20 μM) for 2 and 6 hours showed a robust and significant increase in MLC phosphorylation ($n = 4$), with the response being associated with an increase in actin stress fibers (Figs. 2A, 2B), as we have shown previously.[9] Additionally, consistent with our previous observations,[9] LPA-induced increases in actin stress fibers and MLC phosphorylation correlated well with increased focal adhesions based on vinculin distribution (not shown) and significantly elevated levels of phosphorylated focal adhesion kinase (Fig. 2C; $n = 4$). To determine the relative importance of PKC, Rho kinase, and MLCK in LPA-driven increases in HTM cell contractile activity, confluent serum starved HTM cells were pretreated with the respective kinase inhibitors GF109203X (10 μM), Y27632 (1 μM), or ML-7 (20 μM) for 30 minutes and stimulated with LPA (20 μM) for 2 hours prior to evaluating changes in MLC phosphorylation. While LPA failed to stimulate MLC phosphorylation in Y-27632 or ML-7 pretreated HTM cells, it significantly increased MLC phosphorylation in GF109203X pretreated and control HTM cells revealing only a partial involvement of PKC in LPA induced contractile activity relative to Rho kinase and MLCK (Fig. 3). Total MLC protein levels remained unaltered (Fig. 3) under the above-described conditions. Given these differential responses of LPA-mediated MLC phosphorylation to the PKC, Rho kinase, MLCK inhibitors, we used these reagents to modulate contractile activity in HTM cells to evaluate how differences in HTM cell contractility might influence activation of the well-characterized, mechanosensitive transcriptional regulator YAP/TAZ.[39,42]

Association of LPA-Induced TM Cell Contractile Activity With Stimulation of YAP/TAZ Transcriptional Activity, and Expression of CTGF and Cyr61

YAP and TAZ are transcription factors known to participate in sensing mechanical cues from the extracellular environment.[34,42] Acting downstream of the Hippo pathway, these transcriptional coactivators regulate the expression of CTGF and Cyr61, which are in turn involved in ECM production and wound healing.[24,32,42,54] To explore the role of YAP and TAZ in LPA-induced changes in the levels of CTGF and Cyr61 in HTM cells, serum-starved HTM cells were treated with LPA (20 μM) for 2 and 6 hours, and evaluated for changes in levels of YAP and TAZ, their phosphorylated forms, and levels of CTGF and Cyr61 by immunoblot analyses (Fig. 4). While the levels of phosphorylated YAP in HTM cell lysates were significantly reduced within 2 hours of LPA treatment compared with control cells, there were no further decreases detected in cells treated with LPA for 6 hours (Fig. 4). On the other hand, the level of total YAP were significantly increased in LPA-treated (2 hours) cells relative to control and HTM cells treated with LPA for 6 hours (Fig. 4A; $n = 4$). Under similar conditions, while the levels of total TAZ were significantly increased in LPA-treated (6 hours) HTM cells, there were no significant changes in levels of p-TAZ. However, both YAP and TAZ showed increased nuclear localization in the LPA-treated (2 hours) HTM cells compared with control cells (Fig. 4B). Partly, as a consequence of the LPA-dependent YAZ/TAZ activation, the levels of both CTGF and Cyr61 were significantly elevated in the LPA-treated (6 hours) HTM cells compared with control cells (Fig. 4A; $n = 4$). The CTGF antibody used in this study detects two closely migrating immunopositive bands representing glycosylated and nonglycosylated forms of CTGF in HTM cell lysates (Fig. 4A). Immunoblots shown in Fig. 4 were normalized to GAPDH.

Based on the differential effects exerted by PKC, Rho kinase, and MLCK inhibition on MLC phosphorylation, a key regulator of cell contractile activity, we evaluated the impact of treating HTM cells with inhibitors of PKC, Rho kinase, and MLCK on LPA-mediated activation of YAP, by monitoring for changes in the levels of p-YAP and YAP. Consistent with the previous observation (Fig. 4), LPA addition to HTM cells for 2 hours resulted in significant decreases of p-YAP levels (in cell lysates), indicating activation of YAP (Fig. 5A), as well as increases in the levels of YAP. HTM cells treated either with PKC, Rho kinase, or MLCK inhibitors alone did not exhibit any changes in the levels of either p-YAP or YAP relative to control cells. In contrast, addition of LPA to HTM cells pretreated with PKC, Rho kinase, or MLCK inhibitors alone revealed that there was a significant decrease in the levels of p-YAP and an increase in total YAP levels only in cells pretreated with PKC inhibitor, relative to the corresponding controls treated with inhibitor alone. While a decreasing trend in the levels of p-YAP was observed in cells pretreated with Rho kinase and MLCK inhibitors before addition of LPA, the changes were not significant relative to the appropriate controls treated with inhibitor alone.

Consistent with our previous observation on the effects of LPA on CTGF and Cyr61 (Fig. 4), the significant LPA-mediated increase in the levels of CTGF and Cyr61 by LPA in HTM cells was confirmed (Fig. 5B; $n = 4$). However, this response was

Investigative Ophthalmology & Visual Science

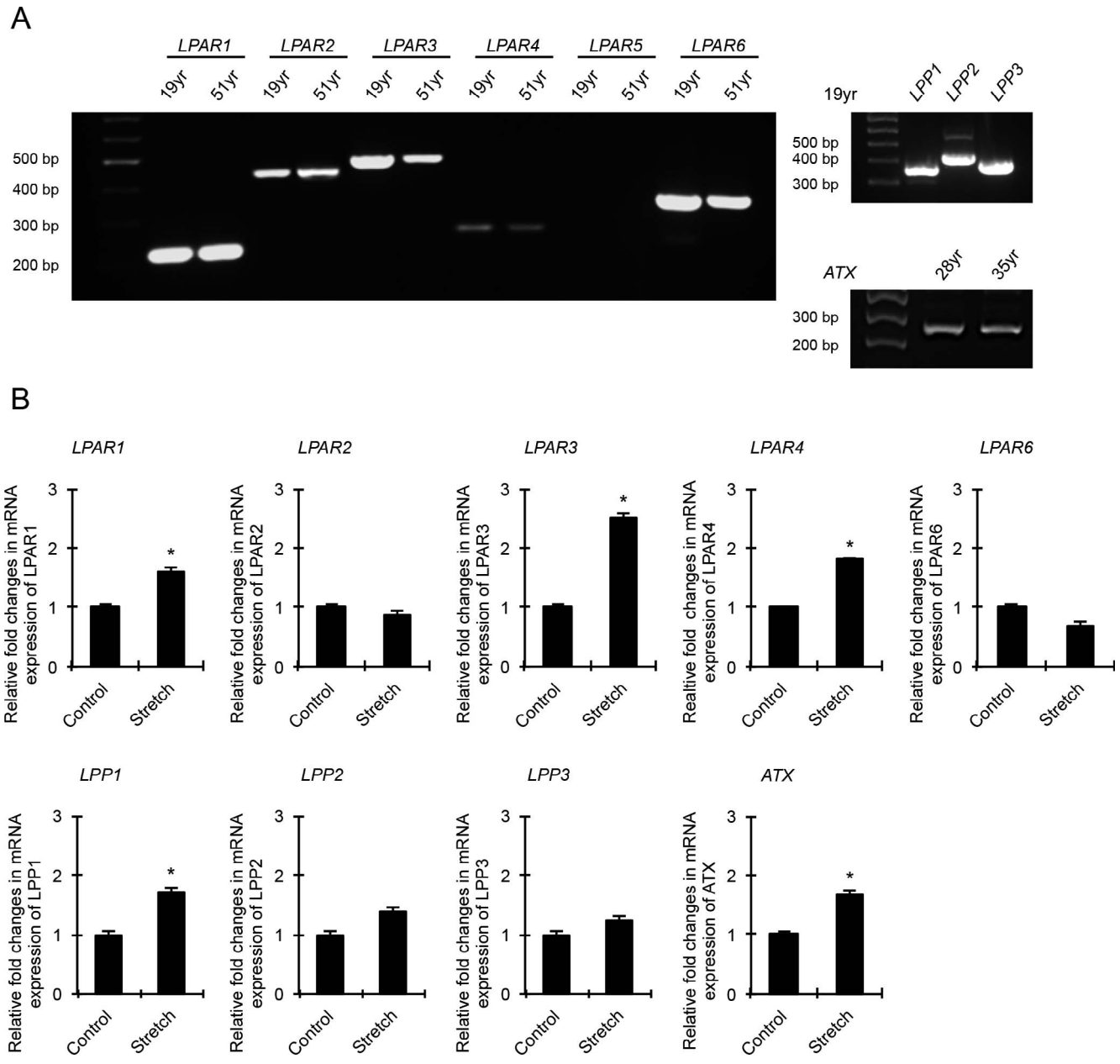

Figure 1. Effects of cyclic mechanical stretch on expression of genes encoding *LPARs*, *LPPs*, and *ATX* in HTM cells. (**A**) RT-PCR–based detection of gene expression profiles for LPA receptors (*LPAR1-6*), *LLPs*, and *ATX* in different HTM cell strains derived from human donors. (**B**) HTM cells subjected to cyclic mechanical stretch (15% stretch, 1 cycle/sec for 24 hours) show significant increase in expression of *LPAR1*, *LPAR3*, *LPAR4*, *LPP1*, and *ATX* genes compared with control cells based on RT-qPCR analysis. Values are mean ± SEM. $n = 6$, $^*P \leq 0.05$.

significantly impaired in the presence of Rho kinase (Y27632) or MLCK (ML-7) inhibitors, but not in the presence of PKC inhibitor (GF109203X), indicating the potential importance of contractile force/tension in the regulation of CTGF and Cyr61 expression (Fig. 5B; $n = 4$).

The Role of LPA Receptors in Regulation of TM Cell Contractile Activity, YAP Activation, and Expression of CTGF and Cyr61 in TM Cells

To understand the regulation of YAP activity and CTGF and Cyr61 expression by LPA receptors in the context of MLC phosphorylation-dependent HTM cell contractile activity, we evaluated the effects of LPA receptor antagonists on LPA-mediated MLC phosphorylation. As expected, serum-starved HTM cells treated with LPA (20 μM) for 2 hours exhibited robust and significant increases in MLC phosphorylation confirming that LPA augments contractile activity and tension in HTM cells (Fig. 6). MLC phosphorylation status in serum starved HTM cells treated for 2 hours with antagonists selective for LPA1 (1 μM AM095), LPA2 (1 μM Cpd 35), or LPA1&3 (10 μM Ki16425) receptors alone was not different relative to that of the respective controls (Fig. 6). However, MLC phosphorylation was completely suppressed in HTM cells pretreated with Ki16425 prior to LPA addition, compared with cells treated with LPA alone, indicating a definitive role for LPA1&3 receptors in the regulation of LPA-induced contractile activity of TM cells (Fig. 6). In contrast, HTM cells pretreated with the

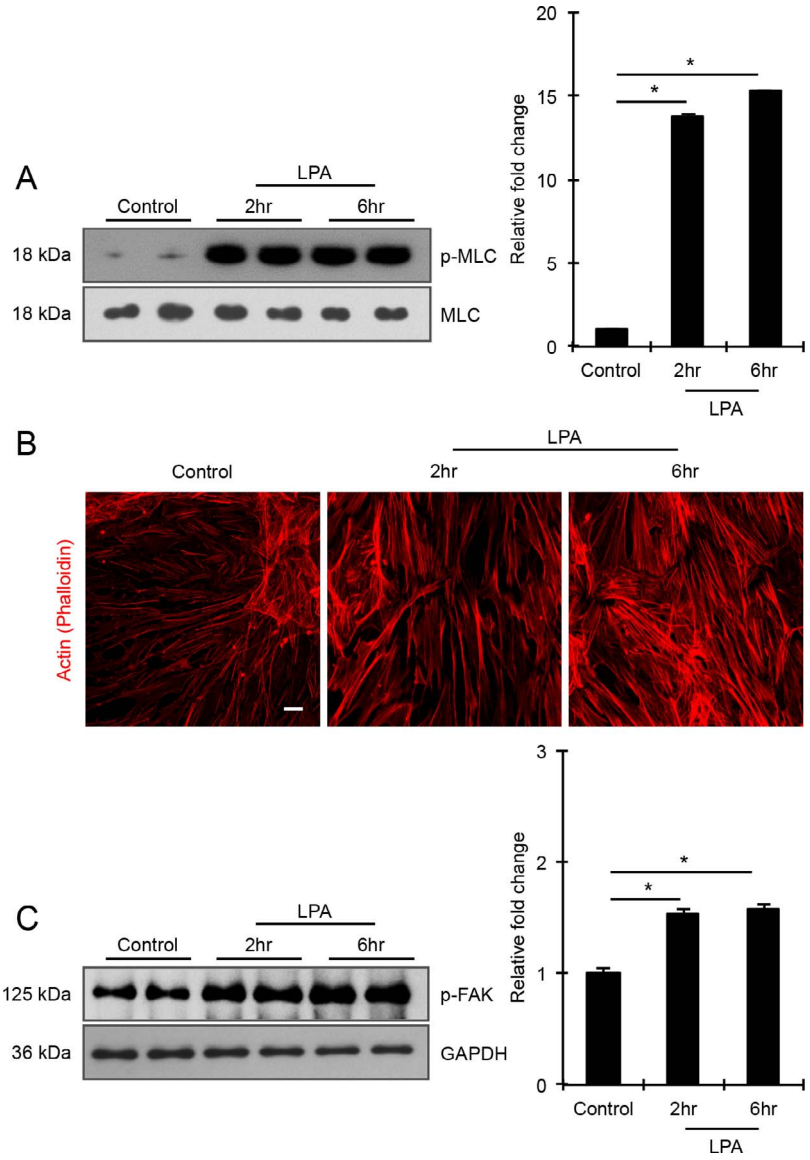

Figure 2. LPA induces formation of actin stress fibers and phosphorylation of MLC and FAK in HTM cells. Serum-starved HTM cells (24 hours) treated with LPA (20 μM for 2 and 6 hours) showed significant increase in the levels of phosphorylated MLC (p-MLC; panel [**A**]) and FAK (p-FAK; panel [**C**]) compared with the control cells, based on quantitative immunoblot analyses. Values are mean ± SEM. $n = 4$, $^*P \leq 0.05$. Changes in p-MLC and p-FAK were normalized to total MLC and GAPDH, respectively. These LPA-induced changes in cell contractility and adhesion were also associated with increased actin stress fiber formation, as evaluated by phalloidin fluorescence staining (**B**). *Scale bar*: 20 μm.

LPA2 receptor antagonist (Cpd 35), showed no difference in the level of LPA-stimulated MLC phosphorylation relative to cells treated with LPA alone. On the other hand, HTM cells pretreated with LPA1 receptor antagonist (AM095) exhibited a significant but not comparable LPA-induced increase in MLC phosphorylation relative to LPA-stimulated controls, indicating a partial involvement of the LPA1 receptor in regulation of LPA-dependent MLC phosphorylation in HTM cells (Fig. 6; $n = 4$). There was no significant difference in levels of total MLC in HTM cells under any of the conditions evaluated in the above studies.

To explore the consequences of the differential involvement of various LPA receptors in MLC phosphorylation, we evaluated the effects of LPA receptor antagonists on YAP activation and expression of CTGF and Cyr61 in HTM cells. As we observed in previous experiments, LPA consistently and significantly decreased the levels of p-YAP with a concomitant increase in total YAP levels in HTM cells, compared with control cells (Fig. 7; $n = 4$). Under these conditions (6 hours), protein levels of both CTGF and Cyr61 were also significantly increased compared with controls (Fig. 7). The levels of p-YAP in HTM cells treated with antagonists of LPA1 (AM095), LPA2 (Cpd 35), or LPA1&3 (Ki16425) receptors alone were not significantly different from corresponding controls (Fig. 7A). However, pretreatment of HTM cells with LPA2-selective antagonist (Cpd 35) did not impact the LPA-induced decrease in p-YAP or increase in total YAP levels, or the increase in levels of CTGF and Cyr61, relative to control cells stimulated with LPA alone (Fig. 7B). On the other hand, pretreatment of HTM cells with LPA1 or LPA1&3 receptor antagonists prior to LPA stimulation resulted in lower levels of total YAP as well as CTGF and Cyr61 relative to controls stimulated with LPA alone (Fig. 7B). P-YAP levels in AM095 or Ki16425 pretreated, LPA-stimulated HTM cells were found to be higher compared with cells stimulated with LPA alone. Collectively, these results also suggest that mainly LPA1&3 receptor–mediated increases in

Investigative Ophthalmology & Visual Science

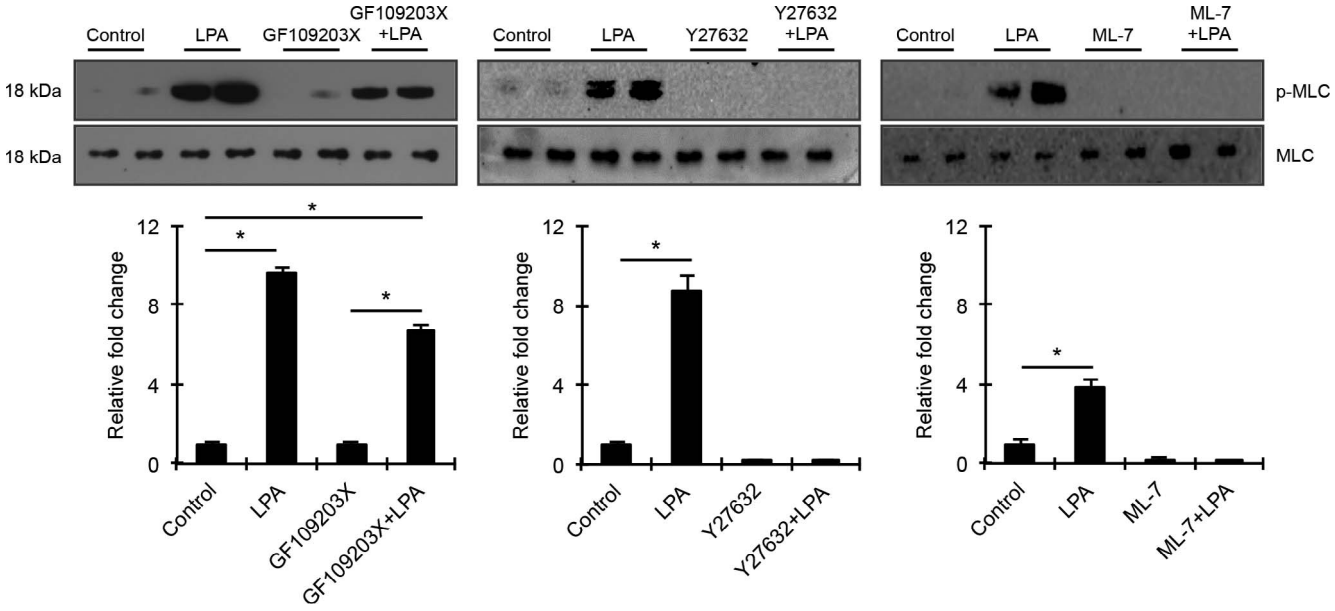

Figure 3. Differential regulation of HTM cell contractility by PKC, Rho kinase, and MLCK. To determine the relative role of PKC, Rho kinase, and MLC kinase in LPA-induced contractile activity, serum-starved HTM cells were pretreated with specific inhibitors of Rho kinase (1 μM Y27632), PKC (10 μM GF109203X), MLCK (20 μM ML-7), or with DMSO control for 30 minutes prior to stimulation with LPA (20 μM for 2 hours). HTM cells treated with LPA exhibited a robust and significant increase in MLC phosphorylation compared with control cells. Unlike Rho kinase and MLCK inhibitors, which completely suppressed LPA-stimulated increases in MLC phosphorylation, the PKC inhibitor only partially reduced LPA-induced increases in MLC phosphorylation. Changes in p-MLC protein levels were normalized to total MLC protein. Histograms depict the relative increase in p-MLC levels relative to control cells. Values are mean ± SEM. $n = 4$, $^*P \leq 0.05$.

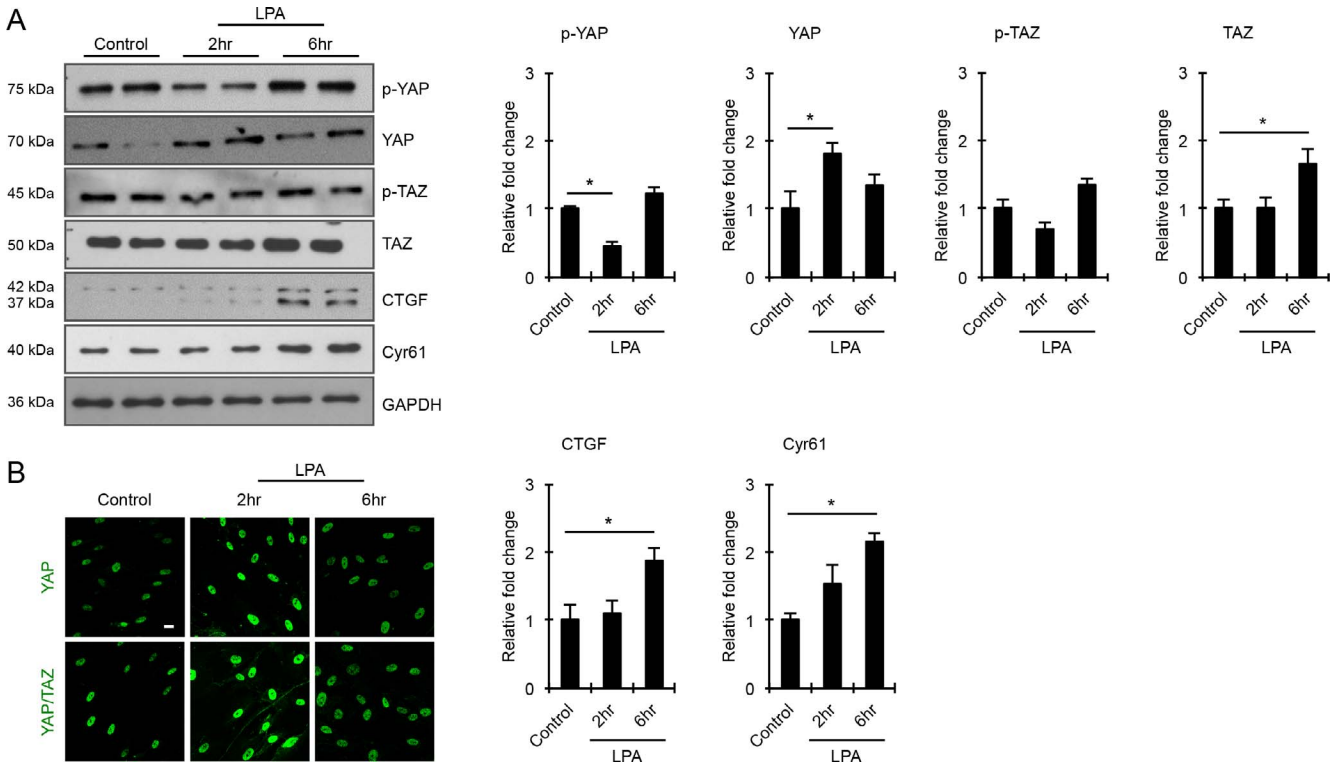

Figure 4. LPA-induced activation of YAP/TAZ transcription factors associates with elevated levels of CTGF and Cyr61 in HTM cells. (**A**) Serum-starved HTM cells stimulated with LPA (20 μM) for 2 and 6 hours showed significantly decreased levels of phospho-YAP and increased levels of total YAP after 2 hours of treatment compared with control cells. In the case of TAZ in contrast, only total TAZ levels were significantly increased in HTM cells stimulated with LPA for 6 hours, relative to control cells. Under these treatment conditions (6 hours), the levels of both CTGF and Cyr61 were significantly increased in HTM cells compared with control cells. Values shown in histograms are based on $n = 4$ samples and presented as mean ± SEM. Data were normalized to GAPDH loading control. (**B**) Stimulation of HTM cells with LPA (20 μM) for 2 hours led to increased YAP/TAZ nuclear accumulation compared with control cells, based on immunofluorescence imaging analysis. *Scale bar*: 20 μm.

Investigative Ophthalmology & Visual Science

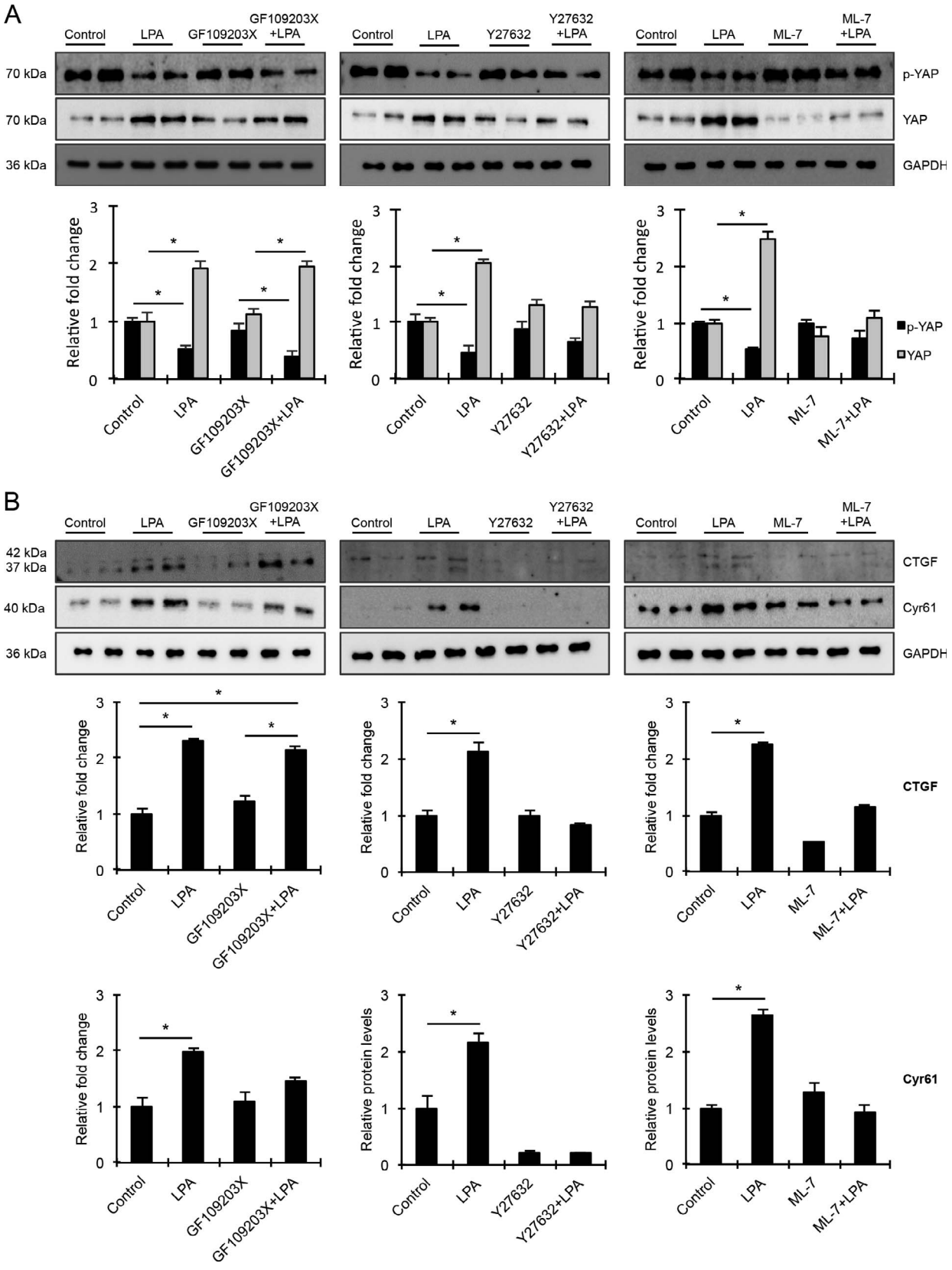

Figure 5. Differential influence of PKC, Rho kinase, and MLCK inhibition on the activation of mechanosensing YAP/TAZ transcription factors, and on levels of CTGF and Cyr61. To determine how the differential effects of PKC, Rho kinase, and MLC kinase inhibitors on contractile activity in HTM cells (Fig. 3) impacts activation of YAP and TAZ transcription factors in these cells, HTM cells were pretreated with specific inhibitors of PKC (10 μM GF109203X), Rho kinase (1 μM Y27632), MLCK (20 μM ML-7), or with DMSO (control cells) for 30 minutes, prior to LPA addition (20 μM) for 2 hours. (**A**) As shown before in Figure 4, LPA alone stimulated a significant decrease in p-YAP levels and stimulated an increase in the levels of total YAP relative to the corresponding controls. Treatment with any of the inhibitors alone was without effect for all parameters evaluated. Pretreatment

of HTM cells with GF109203X prior to LPA addition caused only partial suppression of LPA-mediated decrease in p-YAP levels and increase in total YAP levels relative to controls treated with inhibitor alone. In contrast, cells pretreated with Rho kinase or MLCK inhibitors prior to LPA stimulation did not exhibit changes either in the levels of p-YAP or total YAP compared with cells treated with the respective kinase inhibitors alone. (**B**) As shown before in Figure 4, LPA alone (6 hours) significantly increased the levels of both CTGF and Cyr61 compared with control cells. In addition, HTM cells pretreated with Rho kinase or MLCK inhibitors (30 minutes) prior to LPA (6 hours) stimulation did not exhibit differences in the levels of CTGF and Cyr61 compared with the cells treated with the respective inhibitors alone. In contrast, LPA stimulated a significant increase in CTGF levels in HTM cells pretreated with PKC inhibitor relative to cells treated with inhibitor alone. While cells pretreated with the PKC inhibitor before LPA addition exhibited an increased trend in Cyr61 levels relative to controls treated with the kinase inhibitor alone, this difference was not statistically significant. Values are shown as mean ± SEM, $n = 4$ and $^*P \leq 0.05$. The immunoblot data were normalized with GAPDH.

cell tension due to augmented contractile activity regulate YAP transcriptional activity and expression of CTGF and Cyr61 in HTM cells.

LPA Induced ECM Production in TM Cells

Having found that LPA activates YAP activity in concert with increased contractile activity, and increases the levels of fibrogenic factors CTGF and Cyr61 in HTM cells, we probed the expression levels of specific ECM proteins and α-SMA by immunoblotting and immunofluorescence analyses in LPA-treated HTM cells. For this, serum starved HTM cells were treated with LPA (20 μM) for 6 hours and cells were either fixed for immunofluorescence or processed to generate cell lysate (800*g* supernatants) for immunoblotting analysis. LPA-treated HTM cells showed significantly increased levels of α-SMA, laminin, collagen type I, and fibronectin compared with control cells (Fig. 8A). Immunoblots are shown for two individual samples from both control and LPA-treated cells in Figure 8A, and histograms represent values based on four replicate observations (Fig. 8B). Consistent with the immunoblotting results, LPA-treated cells also showed a notable increase in immunofluorescence for α-SMA, laminin, collagen type I, and fibronectin compared with controls (Fig. 8B). Images were recorded under identical magnification settings for both test and control cells.

In addition to the early effects of LPA on expression of selected ECM proteins, we also evaluated differential expression of ECM protein profiles in HTM cells treated with LPA for 48 hours by quantitative proteomics analysis using LC-MS/MS mass spectrometry. For this, serum-starved HTM cells were treated with 5 μM LPA added twice a day, for a total of 48 hours. Due to the known rapid hydrolysis of LPA by LPPs,[16] a repeat addition of fresh LPA was performed. Control cells were similarly treated with vehicle containing ethanol. Following treatment, the cell monolayer was decellularized to isolate the ECM-enriched fraction, which was then processed to extract both, the SDS/urea soluble and SDS/urea insoluble ECM fractions as described in the Methods section. Both types of ECM fractions were subjected to tryptic digestion and subsequently to LC-MS/MS. This analysis was carried out with two independent TM cell strain samples, and for each sample, ECM fractions from cells grown in and processed from two separate petri plates were pooled. Tables 2 and 3 list the HTM-cell ECM and ECM-associated proteins that exhibited a minimum of 1.5-fold increase with LPA treatment over controls, in the SDS/urea soluble and insoluble fractions, respectively, for two individual samples. As shown in Tables 2

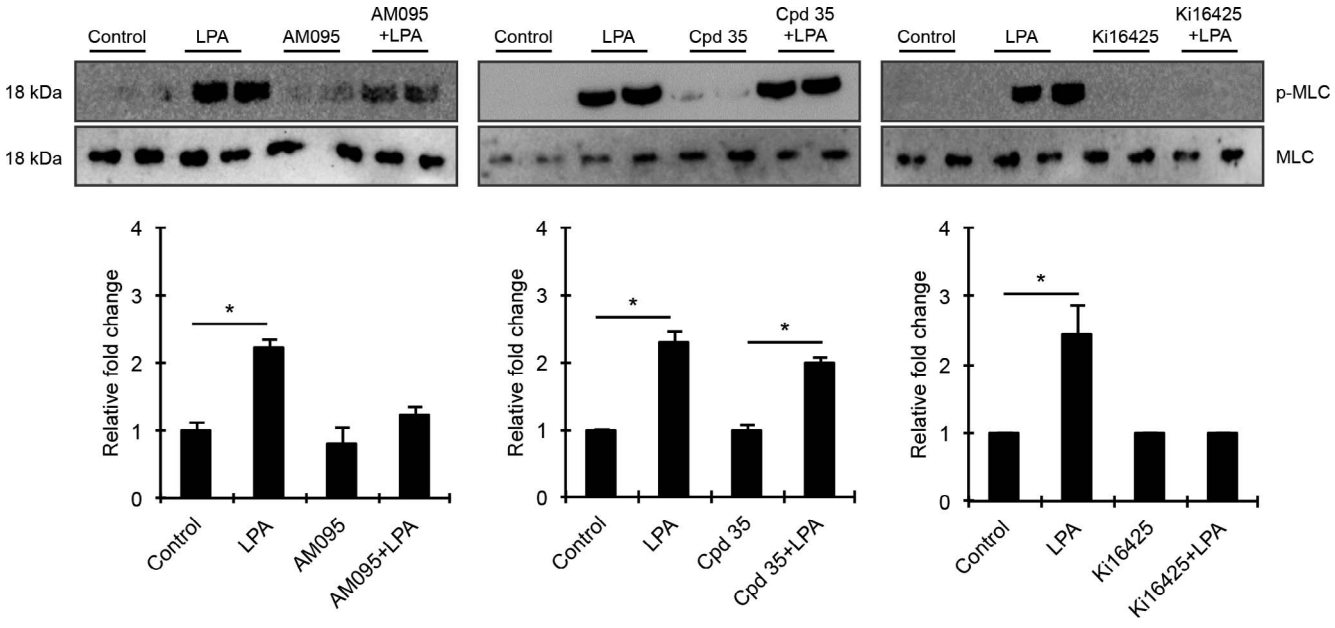

Figure 6. Differential involvement of LPA receptors in regulation of HTM cell contractile activity. To determine the role of LPA receptors in HTM cell contractile activity, serum-starved HTM cells were treated either with LPA (20 μM for 2 hours) alone, or pretreated with LPA receptor antagonists (LPA1: 1 μM AM095; LPA2: 1 μM Cpd 35, or LPA1&3: 10 μM Ki16425) for 30 minutes, followed by LPA addition, or treated with LPA receptor antagonist (2 hour) alone. As shown earlier (Fig. 3), LPA induced a robust and significant increase in the levels of p-MLC compared with control cells, and while this response was completely blocked in the presence of Ki16425, Cpd 35 was without effect. On the other hand, AM095 partially but significantly reduced the levels of p-MLC in the presence of LPA compared with cells treated with LPA alone. The levels of total MLC were not found to be different relative to corresponding control cells, for any of the treatments described above. Immunoblot data for p-MLC were normalized to total MLC. Values are mean ± SEM, $n = 4$ and $^*P \leq 0.05$.

Investigative Ophthalmology & Visual Science

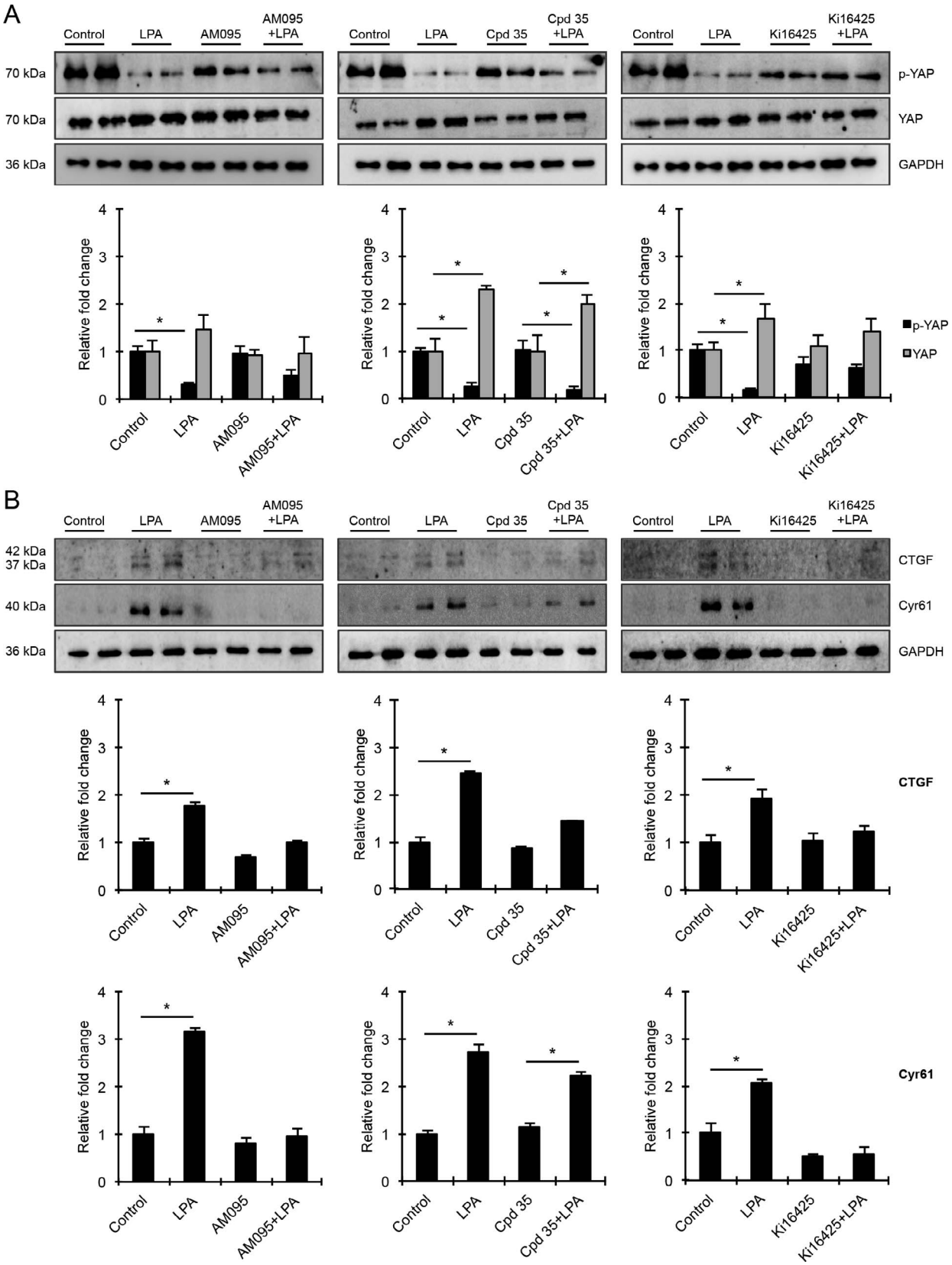

Figure 7. Differential effects of LPA receptor antagonists on YAP activation and the levels of CTGF and Cyr61 in HTM cells. (**A**) Serum-starved HTM cells were treated either with LPA (20 μM, 2 hours) alone, or pretreated with LPA receptor antagonists (LPA1: 1 μM AM095; LPA2: 1 μM Cpd 35 or LPA1&3: 10 μM Ki16425; 30 minutes) prior to addition of LPA, or treated with LPA receptor antagonists (2 hours) alone. As shown in Figures 4 and 5, LPA stimulation induced a consistent and significant decrease in levels of p-YAP and an increase in the total YAP compared with control cells. These effects were abolished in cells pretreated with LPA1 and LPA 1&3 receptor antagonists prior to LPA stimulation, but not in cells pretreated with LPA2 receptor antagonist. (**B**) Under the above-described conditions, LPA stimulation also stimulated a significant increase in the levels of CTGF and Cyr61 relative to the corresponding controls treated with inhibitor alone, which was suppressed by pretreatment with LPA1 or LPA1&3 receptor antagonists, but not with LPA2 receptor antagonist. Immunoblot data were normalized to GAPDH. Values are mean ± SEM, $n = 4$ and $^*P \leq 0.05$.

Investigative Ophthalmology & Visual Science

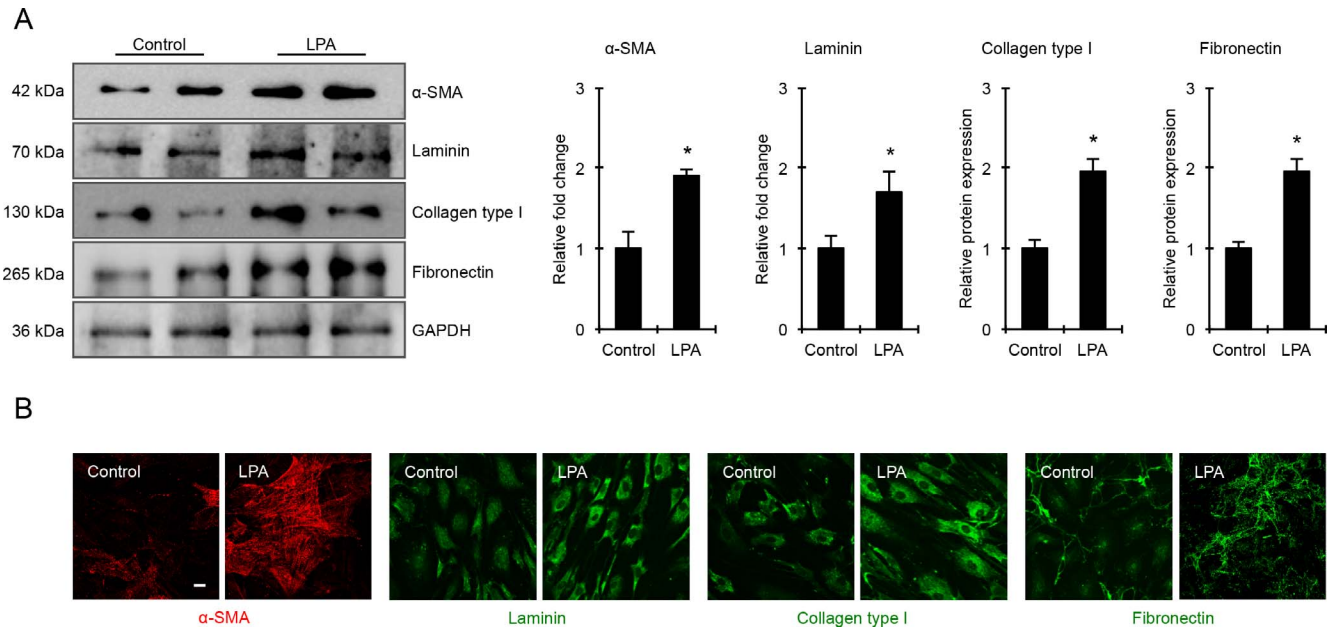

Figure 8. LPA increases α-SMA and ECM production in HTM cells. (**A**) Cell lysates (10 μg protein) derived from serum-starved HTM cells treated with LPA (20 μM for 6 hours) showed significantly increased levels of α-SMA, laminin, collagen type I, and fibronectin compared with control cells based on immunoblotting analyses. Histograms represent values (mean ± SEM) derived from four replicate analyses. $^*P \leq 0.05$. This observation was further confirmed by immunofluorescence analysis as shown in panel (**B**). Representative confocal images of immunostained cells treated with LPA (6 hours) show relatively higher staining for α-SMA, laminin, collagen type I, and fibronectin compared with the control cells. *Scale bar*: 20 μm.

and 3, various ECM proteins were elevated in LPA treated HTM cells, with many more ECM proteins exhibiting increased levels in the SDS/urea insoluble fraction relative to the SDS/urea-soluble fractions derived from LPA-treated cells. Notable ECM proteins exhibiting LPA-induced increases in expression, included collagen type I, fibronectin, laminin, fibulin, fibrillin, decorin, periostin, sushi repeat-containing protein SRPX2, thrombospondin, vitronectin, biglycan, and EGF-containing fibulin-like extracellular matrix protein.

For secondary confirmation, the SDS/urea-soluble ECM fractions derived from LPA-treated and control HTM cells described above were subjected to immunoblot analysis and as shown in Figure 9A, the levels of laminin, collagen type I, and fibronectin were found to be robustly elevated in LPA-treated HTM cells. These data were further supported by immunofluorescence analysis for laminin, fibronectin, and collagen type I in LPA-treated HTM cells (Fig. 9B). For loading control, equal amounts of SDS/urea-soluble fractions were separated by SDS-PAGE and stained with gel code blue, following which one of the protein bands was used for normalization.

Table 2. LPA-Induced ECM Proteins (SDS/Urea Soluble Fraction) in HTM Cells

Identified Proteins	Accession Number	Sample 1	Sample 2
Collagen alpha-1 (VI) chain	CO6A1		*
Collagen alpha-1 (XVIII) chain	COIA1	*	
Collagen alpha-3 (VI) chain	CO6A3		*
Fibronectin	FINC	*	*
Filamin-A	FLNA	*	*
Laminin subunit gamma-1	LAMC1	*	
Matrix Gla protein	MGP	*	
POTE ankyrin domain family member E	POTEE	*	

* Indicates significant increase (1.5-fold) in sample 1 and sample 2 compared with controls.

Discussion

The broad objective of this study was to expand our molecular understanding of LPA-induced resistance to AH outflow and ocular hypertension.[9] To this end, here we explored how the interrelationship between LPA-induced cellular contractility and the activation of mechanotransducing transcription factors YAP and TAZ influences the expression of profibrotic matricellular (CTGF and Cyr61) and ECM proteins in HTM cells. Our data demonstrate that LPA induces via LPA receptors the activation as well as increases in the levels of YAP and TAZ, and upregulates the expression of CTGF, Cyr61, and various ECM proteins in HTM cells, in an actomyosin-driven contractile force–dependent manner. These experimental observations emphasize the importance of signaling pathways that integrate cell contractile activity, adhesive interactions, and actin cytoskeletal organization with mechanosensitive transcriptional activation of YAP and TAZ to modulate ECM production via proteins of the CNN family (CTGF and Cyr61) and other gene targets in HTM cells. Moreover, our results infer that LPA-induced ECM production via transcriptional activation of YAP/TAZ, could be one of the possible etiologic mechanisms involved in increased resistance to AH outflow in glaucoma patient, because the activity of ATX, which generates LPA from LPC was found to be elevated in the AH of primary open-angle glaucoma patients.[10]

It is becoming increasingly evident that the cells of the AH outflow pathway are mechanosensitive and use complex mechanotransducing pathways for maintaining IOP homeostasis in response to changes in IOP and ECM rigidity within the

Investigative Ophthalmology & Visual Science

Table 3. LPA-Induced ECM Proteins (SDS/Urea Insoluble Fraction) in HTM Cells

Identified Proteins	Accession Number	Sample 1	Sample 2
ADAMTS-like protein 1	ATL1	*	*
Basement membrane-specific heparan sulfate proteoglycan core protein	PGBM	*	*
Biglycan	PGS1	*	
Cell migration-inducing and hyaluronan-binding protein	CEMIP	*	*
Cluster of Collagen alpha-1(I) chain	CO1A1	*	
Cluster of Collagen alpha-1(IV) chain	CO4A1	*	
Cluster of Peroxiredoxin-1,2	PRDX1	*	
Clusterin	CLUS	*	*
Collagen alpha-1(V) chain	CO5A1	*	
Collagen alpha-1(VI) chain	CO6A1	*	*
Collagen alpha-1(VIII) chain	CO8A1	*	*
Collagen alpha-1(X) chain	COAA1		*
Collagen alpha-1(XII) chain	COCA1	*	
Collagen alpha-1(XVIII) chain	COIA1		*
Collagen alpha-2(I) chain	CO1A2	*	
Decorin	PGS2	*	*
EGF-containing fibulin-like extracellular matrix protein 1	FBLN3		*
Fibrillin-1	FBN1	*	*
Fibronectin	FINC	*	*
Fibulin-1	FBLN1	*	*
Filamin-C	FLNC	*	
Laminin subunit alpha-3	LAMA3		*
Laminin subunit alpha-5	LAMA5		*
Laminin subunit beta-1	LAMB1		*
Laminin subunit gamma-1	LAMC1	*	*
Latent-transforming growth factor beta-binding protein 1	LTBP1	*	*
Latent-transforming growth factor beta-binding protein 2	LTBP2	*	*
Matrix-remodeling-associated protein 5	MXRA5		*
Microfibrillar-associated protein 2	MFAP2		*
Nidogen-1	NID1		*
Procollagen-lysine,2-oxoglutarate 5-dioxygenase 1	PLOD1	*	
Protein S100-A8	S10A8		*
Sushi repeat-containing protein SRPX2	SRPX2	*	
Thrombospondin type-1 domain-containing protein 4	THSD4	*	*
Thrombospondin-1	TSP1	*	*
Versican core protein	CSPG2		*
Vitronectin	VTNC	*	*

* Indicates significant increase (1.5-fold) in Sample 1 and Sample 2 compared to controls.

trabecular outflow pathway.[29,55,56] Mechanosensing pathways that serve to transduce extracellular physical and mechanical cues into intracellular responses, are therefore key levers for regulation and maintenance of IOP and AH outflow.[29,55–59] Because cell adhesive, cell-cell junctional proteins, and their interactions with the actomyosin cytoskeletal proteins are known to play a key role in mechanotransduction-driven transcriptional activation,[3441,42,60] in this study we focused on exploring the effects of LPA on the transcription factors YAP/TAZ and the expression of downstream profibrotic matricellular proteins CTGF and Cyr61 and ECM production. LPA and its receptors regulate diverse cellular activities by activating multiple intracellular signaling mechanisms, cellular contraction, cell adhesive characteristics, and actin cytoskeletal organization, but also transcriptional activity leading to ECM production.[13,17–20,27] LPA has been shown to induce myosin II-associated cellular contraction, formation of actin stress fibers, focal adhesions, calcium signaling, expression of CTGF and α-SMA, and production of ECM proteins in HTM cells.[2,9,21] Perfusion of enucleated eyes with LPA has been reported to increase resistance to AH outflow through the TM.[9,21,30] Because the molecular link between LPA-induced HTM cell contractile activity and transcriptional activity is not thoroughly understood however,[22] we addressed this aspect in the current study.

Importantly, this study confirmed that the expression of LPARs, LPPs, and ATX is sensitive to cyclic mechanical stretch, indicating a possible role for these proteins in the homeostasis of IOP and AH outflow under IOP fluctuations. Our previous studies have also revealed an association between elevated IOP, HTM tissue contractility, and Rho GTPase activation.[57] Because HTM cell contraction is known to be regulated by several kinases including the PKC, Rho kinase, and MLCK,[2,61] we evaluated the relative contributions of these kinases toward LPA-mediated MLC phosphorylation in HTM cells. Our studies demonstrate that MLCK and Rho kinase inhibitors abolished, while PKC inhibition partially suppressed the LPA-stimulated increase in MLC phosphorylation, implying that MLCK and Rho kinase play a dominant role in regulating LPA-induced HTM cell contraction. Taking advantage of the observed differential effects of these kinase inhibitors on HTM cell contraction, we proceeded to evaluate their effects on YAP/TAZ activation. LPA stimulation of serum-starved HTM cells led to a decrease in the levels of p-YAP, with a concomitant increase in the levels of total YAP and TAZ. The levels of CTGF and Cyr61, both of which are known transcriptional targets of YAP/TAZ, increased significantly under these conditions, suggesting the upregulation of YAP/TAZ transcriptional activity by LPA in HTM cells, consistent with the known role of LPA in YAP/TAZ activation in other cell types.[17,27,43] We then analyzed the effects of PKC, Rho kinase, and MLCK inhibitors on YAP activation and CTGF and Cyr61 protein levels in LPA-treated HTM cells and found that while inhibition of Rho kinase and MLCK abolished LPA-mediated activation of YAP, increase in YAP, CTGF, and Cyr61 protein levels, PKC inhibition did not significantly attenuate any of these responses. These observations indicate the existence of a close relationship between LPA-mediated increase in HTM contractile force, stimulation of YAP/TAZ transcriptional activation, and upregulation of CTGF and Cyr61 expression.

Because LPA mediates its effects through different G-protein coupled receptors,[13,18] we used selective pharmacologic antagonists of LPA1, 2, and 1&3 receptors to obtain independent and complementary support for the existence of an interrelationship between HTM cell contractile activity and YAP/TAZ transcriptional activation. Pharmacologic antagonism of LPA1, 2, and 3 receptors also resulted in differential effects on LPA-mediated MLC phosphorylation, YAP activation, and

Investigative Ophthalmology & Visual Science

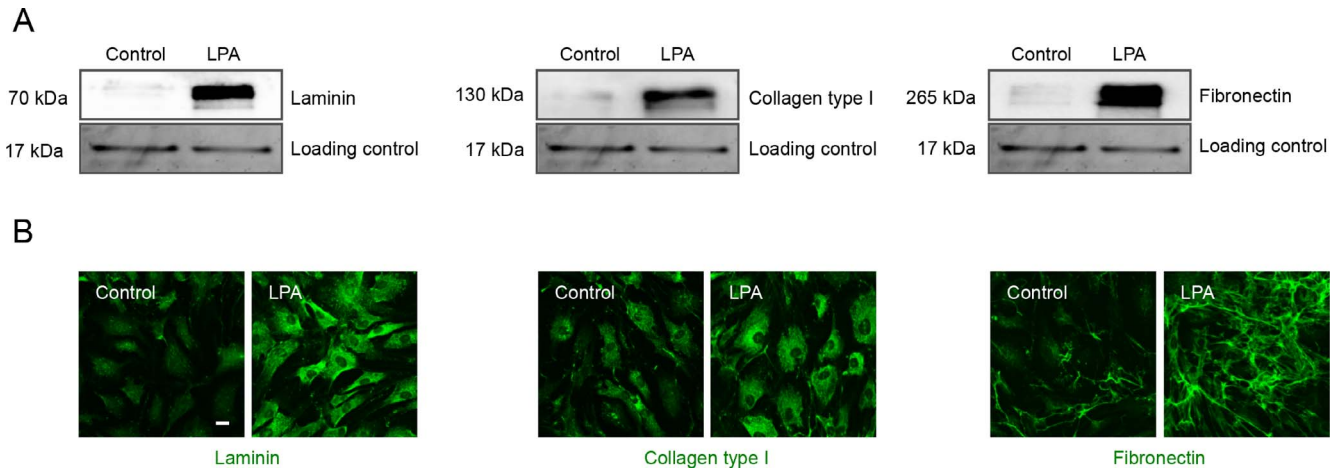

Figure 9. LPA increases ECM production in HTM cells. The ECM-enriched extracellular protein fraction (SDS-urea soluble) derived from HTM cells treated with LPA (5 μM, twice per day) for a total of 48 hours, showed a significant increase in laminin, collagen type I, and fibronectin protein levels compared with control cells. Immunoblots were normalized to one of the protein bands present in the same sample (10 μg) separated by SDS-PAGE and stained using gel code blue. Under the same treatment conditions described above, HTM cells grown on glass cover slips showed a relatively intense staining for the respective proteins (laminin, collagen type I, and fibronectin) relative to controls. *Scale bar*: 20 μm.

CTGF and Cyr61 expression in HTM cells. While LPA1 and LPA1&3 receptor antagonists suppressed LPA-induced MLC phosphorylation and YAP activation-dependent increase in levels of CTGF and Cyr61, LPA2 receptor antagonist (Cpd 35) was almost without effect. Collectively, the differential effects of pharmacologic inhibition of Rho kinase, PKC, MLCK, and LPA1, 2, and 1&3 receptor antagonists on LPA-induced MLC phosphorylation, YAP activation, levels of YAP, CTGF, and Cyr61 in HTM cells reveal that the regulation of HTM cell contractile force by LPA and other physiologic agents known to regulate MLC phosphorylation in HTM cells, including TGF-β, endothelin-1, lipid growth factors, angiotensin II, ECM, and thromboxane A2, very likely activate the YAP/TAZ transcriptional response and other transcriptional mechanisms leading to increased expression of *CTGF* and *Cyr61* and other genes (Fig. 10).[9,20,22,62–64]

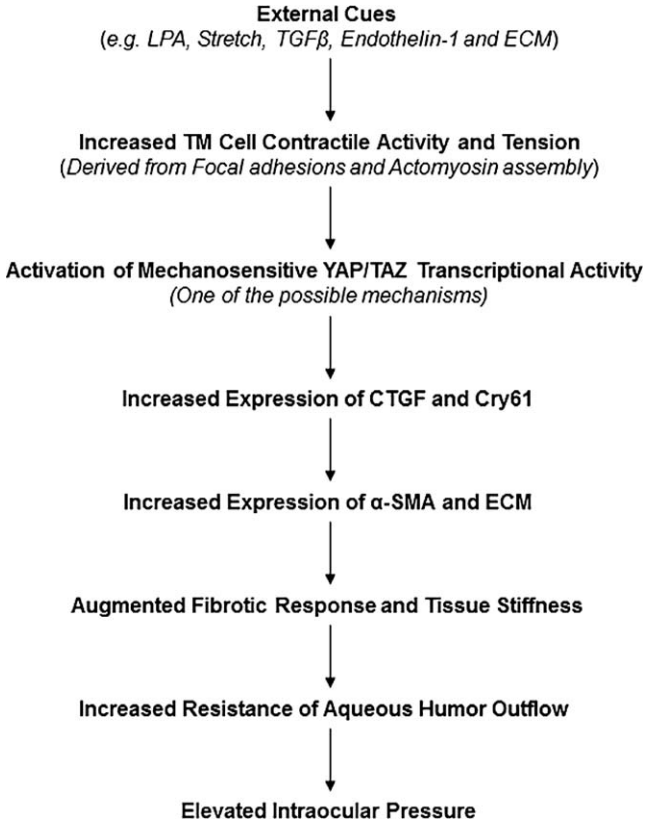

Figure 10. Schematic drawing depicting the interrelationship between LPA-mediated actomyosin associated contractile force and stimulation of mechanosensing YAP/TAZ transcription activity in HTM cells, and the collective contribution of these events toward regulation of CTGF, α-SMA, and ECM protein expression, and AH outflow and IOP. In this scheme, we have not shown the known effects of LPA and LPARs on the Hippo pathway, LATS kinase activity, and YAP/TAZ phosphorylation.[17,27,43]

Additionally, in this study, we have obtained convincing data to support the conclusion that LPA induces the production of various ECM proteins by HTM cells, as evidenced by the elevated levels of fibronectin, collagen type I, laminin, and others by both immunoblotting and quantitative proteomics analyses. As we have shown earlier,[21] LPA treatment of HTM cells increases the levels of α-SMA, the expression of which is regulated partly by an actin polymerization–dependent SRF/MRTF transcriptional mechanism.[17,44,65] Therefore, it is reasonable to conclude that regulation of TM contractile activity, cell adhesion, and actin polymerization by various external factors and intracellular mechanisms can directly modulate expression of CTGF, α-SMA, ECM proteins, and cell plasticity. By extension, it is expected that these key mechanosensitive pathways are tightly controlled within the AH outflow pathway, because their dysregulation could lead to deregulated mechanotransduction, accumulation of ECM, increased resistance to AH outflow, and ocular hypertension (Fig. 10). In support of the above conclusions, CTGF has also been reported to induce expression of various ECM proteins in TM cells and increase IOP in mice.[7,26] Our study also supports previous observations regarding the effects of ECM stiffness, the actin cytoskeleton and dexamethasone on YAP/TAZ activation in TM cells and AH outflow in both normal and glaucomatous eyes.[28,29,66] Finally, this study provides mechanistic insights into the importance of pharmacologic agents targeting molecules that regulate TM contractile activity, cell-adhesive interactions, YAP/TAZ activation, and fibrogenic activities, to lower IOP in glaucoma patients.

Investigative Ophthalmology & Visual Science

Acknowledgments

The authors thank Harold Erickson from Duke University for providing the laminin polyclonal antibody.

Supported by a grant from the National Institutes of Health (R01EY018590; Bethesda, MD, USA), and by the Roche Postdoctoral Fellowship Program (LTYH; Basel, Switzerland).

Disclosure: **L.T.Y. Ho**, None; **N. Skiba**, None; **C. Ullmer**, None; **P.V. Rao**, None

References

1. Weinreb RN, Aung T, Medeiros FA. The pathophysiology and treatment of glaucoma: a review. *JAMA*. 2014;311:1901–1911.
2. Rao PV, Pattabiraman PP, Kopczynski C. Role of the Rho GTPase/Rho kinase signaling pathway in pathogenesis and treatment of glaucoma: bench to bedside research. *Exp Eye Res*. 2017;158:23–32.
3. Tamm ER, Braunger BM, Fuchshofer R. Intraocular pressure and the mechanisms involved in resistance of the aqueous humor flow in the trabecular meshwork outflow pathways. *Prog Mol Biol Transl Sci*. 2015;134:301–314.
4. Tripathi RC, Li J, Chan WF, Tripathi BJ. Aqueous humor in glaucomatous eyes contains an increased level of TGF-beta 2. *Exp Eye Res*. 1994;59:723–727.
5. Wiederholt M, Thieme H, Stumpff F. The regulation of trabecular meshwork and ciliary muscle contractility. *Prog Retin Eye Res*. 2000;19:271–295.
6. Browne JG, Ho SL, Kane R, et al. Connective tissue growth factor is increased in pseudoexfoliation glaucoma. *Invest Ophthalmol Vis Sci*. 2011;52:3660–3666.
7. Junglas B, Kuespert S, Seleem AA, et al. Connective tissue growth factor causes glaucoma by modifying the actin cytoskeleton of the trabecular meshwork. *Am J Pathol*. 2012;180:2386–2403.
8. Gottanka J, Chan D, Eichhorn M, Lutjen-Drecoll E, Ethier CR. Effects of TGF-beta2 in perfused human eyes. *Invest Ophthalmol Vis Sci*. 2004;45:153–158.
9. Mettu PS, Deng PF, Misra UK, Gawdi G, Epstein DL, Rao PV. Role of lysophospholipid growth factors in the modulation of aqueous humor outflow facility. *Invest Ophthalmol Vis Sci*. 2004;45:2263–2271.
10. Iyer P, Lalane R III, Morris C, Challa P, Vann R, Rao PV. Autotaxin-lysophosphatidic acid axis is a novel molecular target for lowering intraocular pressure. *PLoS One*. 2012;7:e42627.
11. Honjo M, Igarashi N, Kurano M, et al. Autotaxin-lysophosphatidic acid pathway in intraocular pressure regulation and glaucoma subtypes. *Invest Ophthalmol Vis Sci*. 2018;59:693–701.
12. Wang H, Edwards G, Garzon C, Piqueras C, Bhattacharya SK. Aqueous humor phospholipids of DBA/2J and DBA/2J-Gpnmb(+)/SjJ mice. *Biochimie*. 2015;113:59–68.
13. Sheng X, Yung YC, Chen A, Chun J. Lysophosphatidic acid signalling in development. *Development*. 2015;142:1390–1395.
14. Aikawa S, Hashimoto T, Kano K, Aoki J. Lysophosphatidic acid as a lipid mediator with multiple biological actions. *J Biochem*. 2015;157:81–89.
15. van Meeteren LA, Moolenaar WH. Regulation and biological activities of the autotaxin-LPA axis. *Prog Lipid Res*. 2007;46:145–160.
16. Tang X, Benesch MG, Brindley DN. Lipid phosphate phosphatases and their roles in mammalian physiology and pathology. *J Lipid Res*. 2015;56:2048–2060.
17. Yu OM, Brown JH. G protein-coupled receptor and RhoA-stimulated transcriptional responses: links to inflammation, differentiation, and cell proliferation. *Mol Pharmacol*. 2015;88:171–180.
18. Moolenaar WH. Bioactive lysophospholipids and their G protein-coupled receptors. *Exp Cell Res*. 1999;253:230–238.
19. Rao PV. Bioactive lysophospholipids: role in regulation of aqueous humor outflow and intraocular pressure in the context of pathobiology and therapy of glaucoma. *J Ocul Pharmacol Ther*. 2014;30:181–190.
20. Luna C, Li G, Huang J, et al. Regulation of trabecular meshwork cell contraction and intraocular pressure by miR-200c. *PLoS One*. 2012;7:e51688.
21. Pattabiraman PP, Maddala R, Rao PV. Regulation of plasticity and fibrogenic activity of trabecular meshwork cells by Rho GTPase signaling. *J Cell Physiol*. 2014;229:927–942.
22. Pattabiraman PP, Rao PV. Mechanistic basis of Rho GTPase-induced extracellular matrix synthesis in trabecular meshwork cells. *Am J Physiol Cell Physiol*. 2010;298:C749–C763.
23. Tsou PS, Haak AJ, Khanna D, Neubig RR. Cellular mechanisms of tissue fibrosis. 8. Current and future drug targets in fibrosis: focus on Rho GTPase-regulated gene transcription. *Am J Physiol Cell Physiol*. 2014;307:C2–C13.
24. Leask A, Abraham DJ. All in the CCN family: essential matricellular signaling modulators emerge from the bunker. *J Cell Sci*. 2006;119:4803–4810.
25. Muehlich S, Rehm M, Ebenau A, Goppelt-Struebe M. Synergistic induction of CTGF by cytochalasin D and TGFbeta-1 in primary human renal epithelial cells: role of transcriptional regulators MKL1, YAP/TAZ and Smad2/3. *Cell Signal*. 2017;29:31–40.
26. Junglas B, Yu AH, Welge-Lussen U, Tamm ER, Fuchshofer R. Connective tissue growth factor induces extracellular matrix deposition in human trabecular meshwork cells. *Exp Eye Res*. 2009;88:1065–1075.
27. Moroishi T, Park HW, Qin B, et al. A YAP/TAZ-induced feedback mechanism regulates Hippo pathway homeostasis. *Genes Dev*. 2015;29:1271–1284.
28. Thomasy SM, Morgan JT, Wood JA, Murphy CJ, Russell P. Substratum stiffness and latrunculin B modulate the gene expression of the mechanotransducers YAP and TAZ in human trabecular meshwork cells. *Exp Eye Res*. 2013;113:66–73.
29. Raghunathan VK, Morgan JT, Dreier B, et al. Role of substratum stiffness in modulating genes associated with extracellular matrix and mechanotransducers YAP and TAZ. *Invest Ophthalmol Vis Sci*. 2013;54:378–386.
30. Chudgar SM, Deng P, Maddala R, Epstein DL, Rao PV. Regulation of connective tissue growth factor expression in the aqueous humor outflow pathway. *Mol Vis*. 2006;12:1117–1126.
31. Lin KC, Park HW, Guan KL. Regulation of the Hippo pathway transcription factor TEAD. *Trends Biochem Sci*. 2017;42:862–872.
32. Panciera T, Azzolin L, Cordenonsi M, Piccolo S. Mechanobiology of YAP and TAZ in physiology and disease. *Nat Rev Mol Cell Biol*. 2017;18:758–770.
33. Pfleger CM. The Hippo pathway: a master regulatory network important in development and dysregulated in disease. *Curr Top Dev Biol*. 2017;123:181–228.
34. Dupont S. Role of YAP/TAZ in cell-matrix adhesion-mediated signalling and mechanotransduction. *Exp Cell Res*. 2016;343:42–53.
35. Santinon G, Pocaterra A, Dupont S. Control of YAP/TAZ activity by metabolic and nutrient-sensing pathways. *Trends Cell Biol*. 2016;26:289–299.
36. Nardone G, Oliver-De La Cruz J, Vrbsky J, et al. YAP regulates cell mechanics by controlling focal adhesion assembly. *Nat Commun*. 2017;8:15321.

37. Low BC, Pan CQ, Shivashankar GV, Bershadsky A, Sudol M, Sheetz M. YAP/TAZ as mechanosensors and mechanotransducers in regulating organ size and tumor growth. *FEBS Lett*. 2014;588:2663–2670.
38. Zhao B, Wei X, Li W, et al. Inactivation of YAP oncoprotein by the Hippo pathway is involved in cell contact inhibition and tissue growth control. *Genes Dev*. 2007;21:2747–2761.
39. Zhao B, Ye X, Yu J, et al. TEAD mediates YAP-dependent gene induction and growth control. *Genes Dev*. 2008;22:1962–1971.
40. Reddy P, Deguchi M, Cheng Y, Hsueh AJ. Actin cytoskeleton regulates Hippo signaling. *PLoS One*. 2013;8:e73763.
41. Sorrentino G, Ruggeri N, Specchia V, et al. Metabolic control of YAP and TAZ by the mevalonate pathway. *Nat Cell Biol*. 2014;16:357–366.
42. Dupont S, Morsut L, Aragona M, et al. Role of YAP/TAZ in mechanotransduction. *Nature*. 2011;474:179–183.
43. Yu FX, Zhao B, Panupinthu N, et al. Regulation of the Hippo-YAP pathway by G-protein-coupled receptor signaling. *Cell*. 2012;150:780–791.
44. Yu OM, Miyamoto S, Brown JH. Myocardin-related transcription factor A and Yes-associated protein exert dual control in G protein-coupled receptor- and RhoA-mediated transcriptional regulation and cell proliferation. *Mol Cell Biol*. 2016;36:39–49.
45. Yamazaki T, Joshita S, Umemura T, et al. Association of serum autotaxin levels with liver fibrosis in patients with chronic hepatitis C. *Sci Rep*. 2017;7:46705.
46. Bain G, Shannon KE, Huang F, et al. Selective inhibition of autotaxin is efficacious in mouse models of liver fibrosis. *J Pharmacol Exp Ther*. 2017;360:1–13.
47. Tager AM. Autotaxin emerges as a therapeutic target for idiopathic pulmonary fibrosis: limiting fibrosis by limiting lysophosphatidic acid synthesis. *Am J Respir Cell Mol Biol*. 2012;47:563–565.
48. Pradere JP, Klein J, Gres S, et al. LPA1 receptor activation promotes renal interstitial fibrosis. *J Am Soc Nephrol*. 2007;18:3110–3118.
49. Swaney JS, Chapman C, Correa LD, et al. A novel, orally active LPA(1) receptor antagonist inhibits lung fibrosis in the mouse bleomycin model. *Br J Pharmacol*. 2010;160:1699–1713.
50. Maddala R, Skiba NP, Rao PV. Vertebrate lonesome kinase regulated extracellular matrix protein phosphorylation, cell shape, and adhesion in trabecular meshwork cells. *J Cell Physiol*. 2017;232:2447–2460.
51. Hughes CS, Foehr S, Garfield DA, Furlong EE, Steinmetz LM, Krijgsveld J. Ultrasensitive proteome analysis using paramagnetic bead technology. *Mol Syst Biol*. 2014;10:757.
52. Ohata H, Tanaka KI, Maeyama N, et al. Physiological and pharmacological role of lysophosphatidic acid as modulator in mechanotransduction. *Jpn J Pharmacol*. 2001;87:171–176.
53. Ridley AJ. Signal transduction through the GTP-binding proteins Rac and Rho. *J Cell Sci Suppl*. 1994;18:127–131.
54. Wang KC, Yeh YT, Nguyen P, et al. Flow-dependent YAP/TAZ activities regulate endothelial phenotypes and atherosclerosis. *Proc Natl Acad Sci U S A*. 2016;113:11525–11530.
55. Zhou EH, Krishnan R, Stamer WD, et al. Mechanical responsiveness of the endothelial cell of Schlemm's canal: scope, variability and its potential role in controlling aqueous humour outflow. *J R Soc Interface*. 2012;9:1144–1155.
56. Vranka JA, Kelley MJ, Acott TS, Keller KE. Extracellular matrix in the trabecular meshwork: intraocular pressure regulation and dysregulation in glaucoma. *Exp Eye Res*. 2015;133:112–125.
57. Pattabiraman PP, Inoue T, Rao PV. Elevated intraocular pressure induces Rho GTPase mediated contractile signaling in the trabecular meshwork. *Exp Eye Res*. 2015;136:29–33.
58. WuDunn D. Mechanobiology of trabecular meshwork cells. *Exp Eye Res*. 2009;88:718–723.
59. Tumminia SJ, Mitton KP, Arora J, Zelenka P, Epstein DL, Russell P. Mechanical stretch alters the actin cytoskeletal network and signal transduction in human trabecular meshwork cells. *Invest Ophthalmol Vis Sci*. 1998;39:1361–1371.
60. Stutchbury B, Atherton P, Tsang R, Wang DY, Ballestrem C. Distinct focal adhesion protein modules control different aspects of mechanotransduction. *J Cell Sci*. 2017;130:1612–1624.
61. Khurana RN, Deng PF, Epstein DL, Vasantha Rao P. The role of protein kinase C in modulation of aqueous humor outflow facility. *Exp Eye Res*. 2003;76:39–47.
62. Rao PV, Deng P, Sasaki Y, Epstein DL. Regulation of myosin light chain phosphorylation in the trabecular meshwork: role in aqueous humour outflow facility. *Exp Eye Res*. 2005;80:197–206.
63. Zhang M, Maddala R, Rao PV. Novel molecular insights into RhoA GTPase-induced resistance to aqueous humor outflow through the trabecular meshwork. *Am J Physiol Cell Physiol*. 2008;295:C1057–C1070.
64. Nakamura Y, Hirano S, Suzuki K, Seki K, Sagara T, Nishida T. Signaling mechanism of TGF-beta1-induced collagen contraction mediated by bovine trabecular meshwork cells. *Invest Ophthalmol Vis Sci*. 2002;43:3465–3472.
65. Posern G, Treisman R. Actin' together: serum response factor, its cofactors and the link to signal transduction. *Trends Cell Biol*. 2006;16:588–596.
66. Peng J, Wang H, Wang X, Sun M, Deng S, Wang Y. YAP and TAZ mediate steroid-induced alterations in the trabecular meshwork cytoskeleton in human trabecular meshwork cells. *Int J Mol Med*. 2018;41:164–172.

Investigative Ophthalmology & Visual Science